

Original article:

STRUCTURAL AND MOLECULAR CHARACTERIZATION OF LOPINAVIR AND IVERMECTIN AS BREAST CANCER RESISTANCE PROTEIN (BCRP/ABCG2) INHIBITORS

Julia de Paula Dutra¹ , Gustavo Scheiffer¹ , Thales Kronenberger^{2,3} , Lucas Julian Cruz Gomes¹ , Isadora Zanzarini¹ , Kelly Karoline dos Santos¹ , Arun K. Tonduru² , Antti Poso^{2,3} , Fabiane Gomes de Moraes Rego⁴ , Geraldo Picheth⁴ , Glaucio Valdameri¹ , Vivian Rotuno Moure^{1*} 

- ¹ Graduate Program in Pharmaceutical Sciences, Laboratory of Cancer Drug Resistance, Federal University of Parana, Curitiba, PR, Brazil
- ² School of Pharmacy, Faculty of Health Sciences, University of Eastern Finland, P.O. Box 1627, FI-70211 Kuopio, Finland
- ³ (a) Department of Internal Medicine VIII, University Hospital Tuebingen, Otfried-Müller-Strasse 14, Tuebingen DE 72076, Germany
(b) Department of Pharmaceutical and Medicinal Chemistry, Institute of Pharmaceutical Sciences, Eberhard-Karls-Universität, Tuebingen, Auf der Morgenstelle 8, 72076 Tuebingen, Germany
(c) Cluster of Excellence iFIT (EXC 2180) “Image-Guided and Functionally Instructed Tumor Therapies”, University of Tuebingen, 72076 Tuebingen, Germany
(d) Tuebingen Center for Academic Drug Discovery & Development (TüCAD2), 72076 Tuebingen, Germany
- ⁴ Graduate Program in Pharmaceutical Sciences, Federal University of Parana, Curitiba, PR, Brazil

* **Corresponding author:** Vivian Rotuno Moure, Graduate Program in Pharmaceutical Sciences, Laboratory of Cancer Drug Resistance, Federal University of Parana, Curitiba, PR, Brazil. E-mail: vivian.moure@ufpr.br

<https://dx.doi.org/10.17179/excli2023-6427>

This is an Open Access article distributed under the terms of the Creative Commons Attribution License (<http://creativecommons.org/licenses/by/4.0/>).

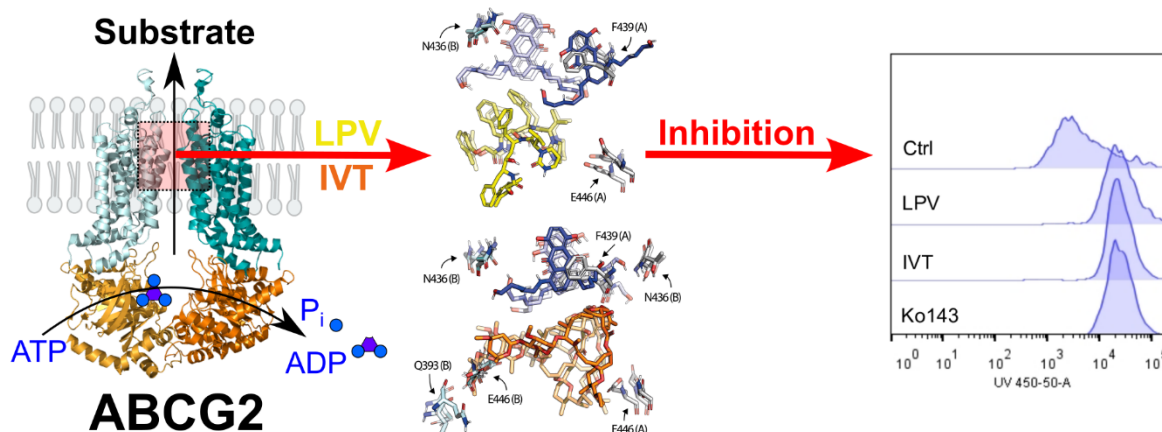


Figure 1: Graphical abstract

ABSTRACT

A current clinical challenge in cancer is multidrug resistance (MDR) mediated by ABC transporters. Breast cancer resistance protein (BCRP) or ABCG2 transporter is one of the most important ABC transporters implicated in MDR and the use of inhibitors is a promising approach to overcome the resistance in cancer. This study aimed to characterize the molecular mechanism of ABCG2 inhibitors identified by a repurposing drug strategy using antiviral, anti-inflammatory and antiparasitic agents. Lopinavir and ivermectin can be considered as pan-inhibitors of ABC transporters, since both compounds inhibited ABCG2, P-glycoprotein and MRP1. They inhibited ABCG2 activity showing IC₅₀ values of 25.5 and 23.4 μM, respectively. These drugs were highly cytotoxic and not transported by ABCG2. Additionally, these drugs increased the 5D3 antibody binding and did not affect the mRNA and protein expression levels. Cell-based analysis of the type of inhibition suggested a non-competitive inhibition, which was further corroborated by *in silico* approaches of molecular docking and molecular dynamics simulations. These results showed an overlap of the lopinavir and ivermectin binding sites on ABCG2, mainly interacting with E446 residue. However, the substrate mitoxantrone occupies a different site, binding to the F436 region, closer to the L554/L555 plug. In conclusion, these results revealed the mechanistic basis of lopinavir and ivermectin interaction with ABCG2.

Keywords: ABCG2, ABCG2 inhibitors, drug repositioning, lopinavir, ivermectin, molecular modelling

INTRODUCTION

Most cancer treatment protocols include chemotherapy, however, the development of resistance is responsible for the lower objective response rate observed with the classical protocols (Gottesman et al., 2016). The development of simultaneous cross-resistance to a wide of structurally unrelated drugs is called multidrug resistance (MDR) (Szakács et al., 2006). The MDR phenomenon in cancer can be categorized as intrinsic (pre-existing) or acquired, triggered by drug exposure (Gottesman, 2002). Different strategies to overcome MDR in cancer have been proposed, albeit it remains an important oncological challenge, since several cellular mechanisms are involved in MDR, including the inactivation of the drug, enhanced DNA repair, mutations or altered expression levels of the biological target, drug compartmentalization, altered mitochondria, failure of programmed cell death and overexpression of ABC transporters (Gottesman et al., 2002; Hall et al., 2009; Szakács et al., 2014).

The human genome encodes 48 ABC proteins, most of them transporters that promote the efflux of substrates mediated by ATP binding and hydrolysis (Dean et al., 2001). ABC transporters show important physiological functions, pumping xenobiotics out of cells to protect them from damage, illustrating their localization in sanctuaries sites in our

body, such as the blood-brain barrier (BBB), blood-testis barrier and blood-placental barrier (Robey et al., 2018). In cancer cells, three ABC transporters are considered most relevant, with undoubted association with chemotherapeutic treatment failure: P-glycoprotein (P-gp or MDR1, encoded by *ABCB1*), multidrug resistance-associated protein 1 (MRP1, encoded by *ABCC1*) and breast cancer resistance protein (BCRP, encoded by *ABCG2*) (Gottesman et al., 2002; Szakács et al., 2006).

ABCG2 was discovered in 1998 by three independent research groups, receiving different names based on the biological model, including BCRP, because of its identification in a breast cancer cell line (Doyle et al., 1998), MXR from resistance caused by mitoxantrone (Miyake et al., 1999) and ABCP, due their presence in placenta (Allikmets et al., 1998). Today, ABCG2 has used to unequivocally announce this transporter. Considering that efflux inhibition consists of the most promising strategy to overcome MDR mediated by ABC transporters, more than a hundred ABCG2 inhibitors have already been identified (Zattoni et al., 2022a). The first described ABCG2 inhibitor was the fungal toxin fumitremorgin C (FTC) (Rabindran et al., 1998). FTC was used as a scaffold for analogues synthesis like Ko143, which is considered a ABCG2 reference inhibitor (Allen et al., 2002). The current list of ABCG2 inhibitors includes several

classes of compounds, including chalcones (Valdameri et al., 2012a), indeno[1,2-*b*]indoles (Kita et al., 2021), stilbenes (Valdameri et al., 2012c), tetrahydroquinoline/4,5-dihydroisoxazole hybrids (Vesga et al., 2021) and chromones (Valdameri et al., 2012b), that can be classified as specific toward ABCG2, dual or pan-inhibitors of ABC transporters (Zattoni et al., 2022a).

Drug repurposing is an interesting and attractive strategy for the rapid identification of ABCG2 inhibitors from existing medicines, that possess distinct molecular targets and have already been identified safe therapeutic agents in humans (Shim and Liu, 2014; Zattoni et al., 2022a). Several classes of drugs already were screened as ABCG2 inhibitors, including antibiotics, antifungals, anti-HIV, calcium channel blockers, glucocorticoids and tyrosine kinase inhibitors (Boumendjel et al., 2011; Juvale and Wiese, 2015; Zattoni et al., 2022a). Among the few potent ABCG2 inhibitors that show IC₅₀ values in the nanomolar range, some were identified by drug repurposing, such as tivozanib, fostamatinib, ponatinib and febuxostat (Zattoni et al., 2022a). In this work, we initially tested the ability of antiviral, anti-inflammatory and antiparasitic drugs that were used to treat COVID-19 to inhibit ABCG2 transporter. Lopinavir and ivermectin have been described as ABC transporters inhibitors (Bierman et al., 2010; Telbisz et al., 2021), but the mechanism of interaction was not characterized, which is important to delineate future pre-clinical experiments.

MATERIAL AND METHODS

Materials

Mitoxantrone, rhodamine 123, GF120918 (Elacridar), Ko143, hydrocortisone, prednisolone, dexamethasone, ivermectin, lopinavir, hydroxychloroquine, chloroquine and oseltamivir and MTT were purchased from Sigma-Aldrich. Hoechst 33342 and TRIzol were purchased from Invitrogen. All other reagents were commercial products of the highest available purity.

Cell cultures

Human HEK293 parental cells (wild-type) and HEK293 cells stably transfected with ABCG2 (HEK293-ABCG2), mouse NIH3T3 parental cells (wild-type) and NIH3T3 cells stably transfected with P-gp (NIH3T3-ABCB1), hamster BHK21 parental cells (wild-type) and BHK21 cells stably transfected with MRP1 (HEK293-ABCC1) were provided by Dr Attilio Di Pietro (IBCP, Lyon, France). All cells were maintained in Dulbecco's Modified Eagle's Medium (DMEM high glucose) supplemented with 10 % fetal bovine serum (FBS), 1 % penicillin/streptomycin, and with 0.75 mg/mL G418 (HEK293-ABCG2), 60 ng/mL colchicine (NIH3T3-ABCB1) or 0.1 mg/mL methotrexate (BHK21-ABCC1) at 37 °C in 5 % CO₂ atmosphere.

Inhibition assay

The ability of drugs to inhibit the transport function of ABC proteins was evaluated using fluorescent substrates by flow cytometry. Cells were aliquoted at a density of 1.0 x 10⁵ cells/tube. Cells were exposed to fluorescent substrates (Hoechst 33342 at 3 μM, rhodamine 123 at 10 μM, calcein-AM at 0.15 μM and mitoxantrone from 2.5 to 25 μM) with or without drugs at different concentrations, and incubated at 37 °C in 5 % CO₂ for 45 min. The cells were centrifuged (2,000 x g for 5 min) and resuspended with 300 μL of cold phosphate buffer saline (PBS) and kept on ice until flow cytometry analysis. Intracellular substrate fluorescence data were acquired using a FACS Celesta (equipped with three lasers: 355, 405 and 488 nm) or a FACS Calibur (equipped with two lasers: 488 and 635 nm) flow cytometer. At least 10,000 events were collected, and the median fluorescence intensities were used for the calculations. The inhibition percentage was calculated using parental cells or a reference inhibitor to achieve 100 % of inhibition. In all experiments, at least three independent replicates were used and IC₅₀ values were calculated by using GraphPad prism software version 6.01.

Cell viability assay

Cells were seeded (2.0×10^4 cells/well) into a 96 wells plate and incubated for 24 h to the attachment. The cells viability was evaluated by MTT (3-[4,5-dimethylthiazol-2-yl]-2,5 diphenyl tetrazolium bromide) assay. Cells were treated with increasing concentrations of drugs for 72 h. After this period, the medium was discarded and the cells monolayer was washed with PBS (100 μ L), followed by incubation at 37 °C with MTT solution (100 μ L of solution 0.5 mg/mL in PBS) for 4 h. Then, the solution was discarded, and the formazan crystals dissolved with 100 μ L of ethanol/DMSO (1:1). The absorbance was measured using a microplate reader at 595 nm (Bio-Rad iMark).

Conformational antibody binding (5D3) assay

The effect of drugs on the binding of a conformational antibody was determined by flow cytometry. HEK293-*ABCG2* cells were cultivated at 37 °C in 5 % CO₂ until approximately 90 % of confluence, then detached and separated in tubes with 5×10^5 cells/tube. Cells were centrifuged at 2,000 x g for 5 min and the supernatant was discarded. The cell pellet was suspended in PBS (100 μ L) containing 40 μ g/mL of BSA. Samples were incubated with inhibitors for 10 minutes at 37 °C. After this period, the primary antibody anti-human *ABCG2* clone 5D3 (BD Pharmingen – dilution 1:100) was added to each sample and incubated for 30 min at 37 °C. Cells were centrifuged and the supernatant was discarded. Cells were suspended in PBS (100 μ L) and the secondary antibody was added (anti-mouse PE, Abcam – dilution 1:200). The samples were incubated at 37 °C for 30 min, centrifuged, and the cell pellet was suspended in 300 μ L of PBS. Data were recorded by flow cytometry. At least 10,000 events were collected.

RT-qPCR

Total RNA was obtained of HEK293-*ABCG2* cells from tissue flasks-25 cm² (at ap-

proximately 90 % of confluence) after treatment for 72 h with lopinavir (6.25 μ M) and ivermectin (1.56 μ M). The total RNA isolation was performed using TRIzol (Invitrogen) protocol according to the manufacturer's instructions. RNA concentration was quantified by absorbance using the NanoDrop™ spectrophotometer and the integrity was evaluated by 1 % agarose gel electrophoresis. RNA was stored at -80 °C. Two micrograms of total RNA were reverse transcribed using High Capacity cDNA Reverse Transcription Kit (Applied Biosystems) according to the manufacturer's instructions, and the resulting cDNA was stored at -20 °C. Using cDNAs as the template, quantitative real-time PCR was performed using the SYBR Green PCR Master Mix (Applied Biosystems) in a 7500™ Real-Time PCR Detection System (Applied Biosystems). A dissociation cycle was performed after each run to check for non-specific amplification or contamination. The mRNA expression levels were normalized using the geNorm 3.4 software, and the corresponding housekeeping gene expression levels. Sets of specific primers were designed using Primer designing tool - NCBI and validated through BLAST and BLAT, and their respective sequences are shown in Table 1. Relative expression levels were estimated using the method described by Pfaffl (2001).

Western blot

Protein was obtained from HEK293-*ABCG2* cells from tissue flasks-25 cm² (at approximately 90 % of confluence) after treatment for 72 h with lopinavir (6.25 μ M) and ivermectin (1.56 μ M) using 200 μ L of RIPA+ buffer and 2 μ L of 0.5 M EDTA pH 8. Protein quantification was performed by Bradford and 40 μ g was separated by gel electrophoresis (8 % polyacrylamide). Proteins were transferred to a PVDF membrane using a semi-dry transference system (GE Healthcare). The membrane was cut in two parts guided by the PageRuler™ Prestained protein ladder. The upper part of the membrane was incubated overnight (4 °C) with *ABCG2* antibody (BXP-21, diluted 1:500) in TBST buffer

Table 1: Nucleotide sequences of primers used for RT-qPCR

| Gene | NCBI reference | Primer sequence | Primer design | Housekeeping genes used by: |
|--------------|----------------|-----------------------------------------------------------|---------------|-------------------------------------------------------------------------------|
| PPIA | NM_021130.5 | F- TAAAGCATACGGGTCCTGGC R- TGCCATCCAACCACTCAGTC | This work | Jacob et al., 2013; Ali et al., 2015; Sharan et al., 2015; Lemma et al., 2016 |
| RPS13 | NM_001017.3 | F- CGTCCCCACTTGGTTGAAGT R- TGAATCTCTCAGGATTACACCGA | This work | Jacob et al., 2013; Zhang et al., 2017) |
| HPRT1 | NM_000194.3 | F- CAGGGATTTGAATCATGTTTGTGT R-ACTCCAGATGTTTCCAAACTCAAC | This work | Potashnikova et al., 2015; Lemma et al., 2016; Saidova et al., 2018 |
| ABCG2 | NM_001257386.2 | F - ATGGTCTGTTGGTCAATCTCAC R – TTATGCTGCAAAGCCGTAATCC | This work | - |

(1.5 M NaCl, 0.5 mM Tris and 0.1 % Tween 20) containing 1 % powdered milk. The lower part of the membrane was incubated overnight (4 °C) with GAPDH antibody (mAB, diluted 1:5000) in TBST buffer containing 1 % powdered milk. The membranes were washed in TBST, and incubated with anti-mouse IgG HRP antibody, diluted 1:2,000 in TBST containing 1 % powdered milk at room temperature for 1 hour. After this incubation, the membranes are washed with TBST. ECL Plus kit substrate (GE Healthcare) was added to the membranes and exposed to a Amersham Hyperfilm (GE Healthcare) for 10 seconds.

Protein selection and preparation for in silico studies

ABCG2 structure with mitoxantrone was retrieved from Protein Data Bank (PDB), PDB ID 6VXI, resolution 3.7 Å (Orlando and Liao, 2020). The structure was prepared and minimized by adding hydrogens, adjusting protonation states (pH 7.4) of amino acids, and fixing missing side-chain atoms using Maestro PrepWizard (version 2021.4). The missing loops between K46 and E60 (N-terminal domain or NTD), S302-P327 (NTD) and G354-Y369 (connecting the transmembrane bundle and the NTD) were generated

using Prime (Jacobson et al., 2004) and the final structure encompassed from A35 to S655.

Molecular docking

Subsequently, the structures had only polar hydrogens maintained and were converted to pdbqt format using the Autodock Tools 1.5.6 (Morris et al., 2009). The ligand structures for ivermectin, lopinavir and mitoxantrone were downloaded from ZINC Database (Sterling and Irwin, 2015), taken into the Avogadro software and subjected to a geometry pre-optimization using the Auto Optimization tool (MMFF94s force field) (Halgren and Nachbar, 1996; Halgren, 1999), followed by visual inspection to ensure that there were no errors. Using Avogadro, the molecule file was prepared for a second geometry optimization in MOPAC2016 (Stewart, 2016), with the semi-empirical quantum PM7 method. At the end of this step, the files were converted to the pdbqt format, also in Autodock Tools, ensuring that all torsions were set to active. For docking, the Autodock Vina 1.2.3 (Eberhardt et al., 2021) was used, in which a grid box was delimited, based on the central region in which the co-crystallized ligand was originally detected. The mitoxantrone + lopinavir (MTX + LPV) and mitoxantrone + ivermectin

(MTX + IVT) docking was performed sequentially, using the 6VXI + MTX docked structure for the inhibitors. The atomic coordinates of the gridbox centroid for all docking experiments were defined as: X = -0.181; Y = -0.222; Z = 0.571, with a 40 Å distance on all three axes. The exhaustiveness parameter was set to 75 and the maximum number of results (poses) to twenty, with a maximum allowed variation of 2 kcal/mol from the first to the last conformation. After, the process was performed with all molecules (substrate and inhibitors), resulting poses served as a starting point for molecular dynamics simulations (MD).

Molecular dynamics simulations

The minimized structures were submitted to MD simulation for further refinement, using a previously published protocol (Zattoni et al., 2022b). Selected docking poses were further validated by MD simulation, where ligand stability within the proposed pocket and its interactions were evaluated. The MD simulations were carried out using the Desmond engine (Bowers et al., 2006) with the OPLS4 force-field (Lu et al., 2021). The simulated system encompassed the protein-ligand complex, a predefined water model (TIP3P; Jorgensen et al., 1983) as a solvent, POPC membranes (automatically positioned according to the alpha-helices), and counterions (Na⁺ or Cl⁻ adjusted to neutralize the overall system charge). The system was treated in an orthorhombic box with periodic boundary conditions specifying the shape and the size of the box as 10x10x13 Å distance from the box edges to any atom of the protein. RESPA integrator time steps of 2 fs for bonded and near, and 6 fs for non-bonded terms far were applied. Short-range coulombic interactions were performed using a time step of 1 fs and a cut-off value of 9.0 Å, whereas long-range coulombic interactions were handled using the Smooth Particle Mesh Ewald (PME) method (Darden et al., 1993). Standard Desmond relaxation protocol was employed. Simulations were run in the NPT ensemble, with a temperature of 310 K (Nosé-Hoover

thermostat) and pressure of 1.01325 bar (Martyna-Tobias-Klein barostat). MD trajectories were visualized, and figures were produced using PyMOL v.2.5 (Schrödinger LCC, New York, NY, USA). At least three independent simulations were performed for each ligand, being 200 ns for inhibitors and 500 ns for mitoxantrone.

Trajectory analyses and MM/GBSA

Protein-ligand interactions were determined using the simulation event analysis pipeline implemented in Maestro (Maestro v2021.4). Distance calculations were performed employing the Maestro event analysis tool (Schrödinger, LLC, New York, NY). The molecular mechanic energies with generalized Born and surface area continuum solvation (MM/GBSA) were calculated with Prime (Jacobson et al., 2004) thermal MM/GBSA script provided by Schrödinger. Each 5th frame of MD was used for MM/GMBSA calculations. Trajectories were clustered according to the ligand's RMSD values in order to select relevant conformations for discussion and figures, using the *trj_cluster.py* script provided by Schrödinger. Figures were generated using PyMOL v2.5 (Schrödinger, LLC, New York, NY).

RESULTS AND DISCUSSION

Identification of lopinavir and ivermectin as ABCG2 inhibitors

In order to identify ABCG2 inhibitors, a repurposing drug strategy utilizing a cell-based model was used. All the eight drugs were selected based on the fact that they were used as therapeutic alternatives for COVID-19, regardless their efficacy. Hydrocortisone, prednisolone, dexamethasone, ivermectin, lopinavir, hydroxychloroquine, chloroquine and oseltamivir were tested to inhibit the activity of ABCG2 in stably transfected HEK293-*ABCG2* cells overexpressing the ABCG2 transporter. This initial screening was performed by flow cytometry using Hoechst 33342 as a fluorescent substrate of ABCG2, and all drugs were essayed at 10 and

100 μM . Only lopinavir and ivermectin inhibited ABCG2 activity (Figure 2A). Both drugs produced a mild inhibition effect at 10 μM , about 25 %. However, a complete inhibition (100 %) was observed at 100 μM (Figure 2A and B). The ABCG2 inhibition caused by lopinavir (Weiss et al., 2007; Bierman et al., 2010) and ivermectin (Jani et al., 2011) was already reported, and most recently, this inhibition effect was confirmed, showing IC_{50} values (compound concentrations giving a

half-maximal inhibition) of ABCG2 inhibition of 13.1 and 3.1 μM , for lopinavir and ivermectin, respectively (Telbisz et al., 2021). Here, we observed IC_{50} values of inhibition of 23.4 and 25.5 μM for lopinavir and ivermectin, respectively (Figure 2C and D). The differences among the IC_{50} values could be associated with the substrate used in each study. Telbisz *et al* have used PhenGreen (PG)-AM as substrate of ABCG2 (Telbisz et al., 2021), while we used Hoechst 33342.

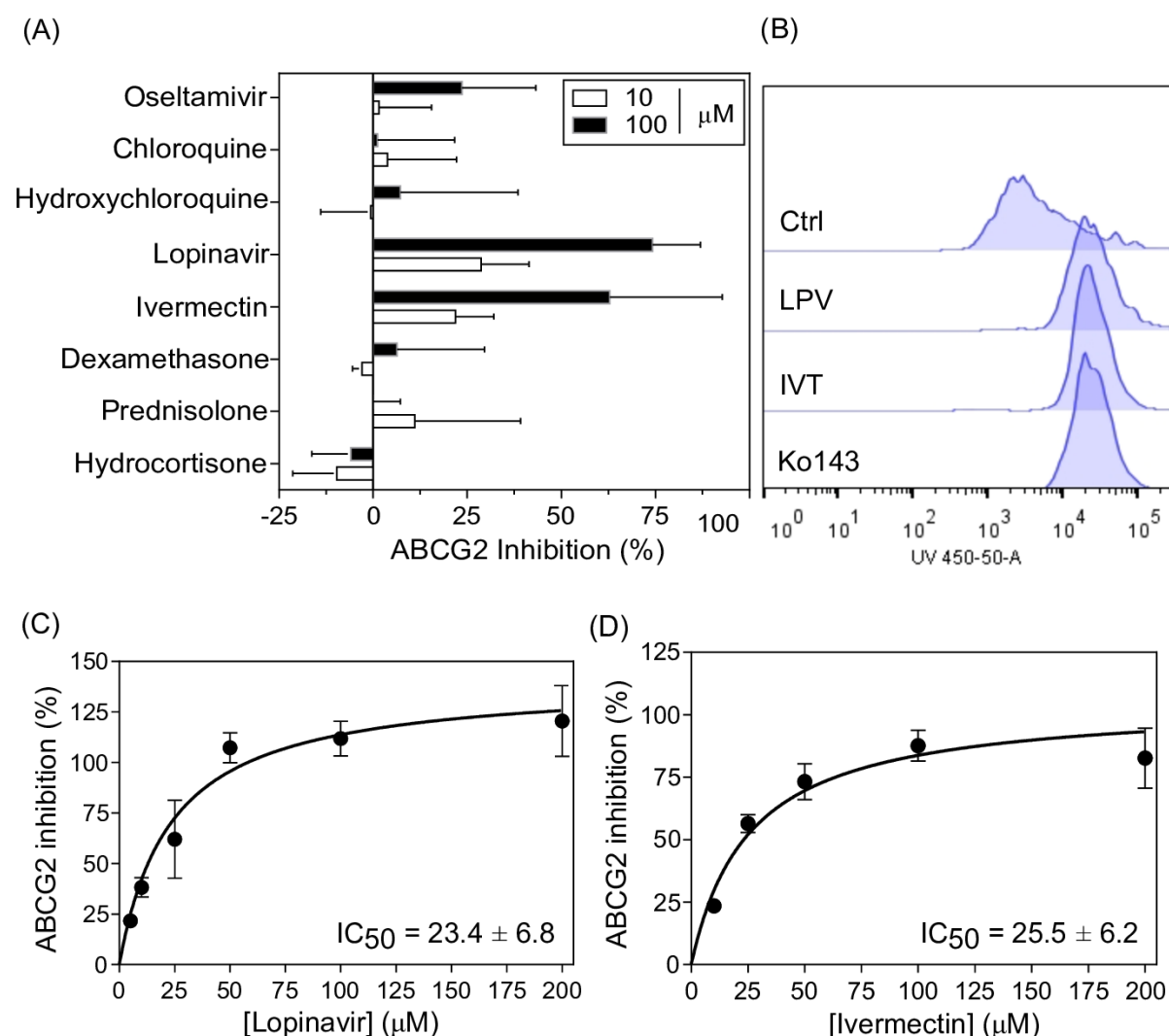


Figure 2: ABCG2 inhibition by flow cytometry. **(A)** Screening of drugs: hydrocortisone, prednisolone, dexamethasone, ivermectin, lopinavir, hydroxychloroquine, chloroquine and oseltamivir as ABCG2 inhibitors. Drugs were tested at 10 and 100 μM on HEK293-ABCG2 cells by flow cytometry using Hoechst 33342 as substrate at 3 μM . Ko143 at 1 μM was used as reference inhibitor (100 % of inhibition). Data represent the mean \pm SD of at least three independent experiments. **(B)** Representative histograms of different conditions, including control (Ctrl) with Hoechst 33342 (3 μM) alone and together with lopinavir (100 μM), ivermectin (100 μM) and Ko143 (1 μM). **(C)** Lopinavir and **(D)** ivermectin IC_{50} curves of ABCG2 inhibition. Data represent the mean \pm SD of at least three independent experiments.

We also investigated the inhibition effect of these eight drugs on P-gp and MRP1 using stably transfected NIH3T3-*ABCB1* cells overexpressing P-gp and BHK21-*ABCC1* cells overexpressing MRP1, respectively. In this case, rhodamine 123 was used as substrate of P-gp and calcein-AM was used as substrate of MRP1. Lopinavir and ivermectin acted as P-gp (see supplementary information Figure 1) and MRP1 (see supplementary information Figure 2) inhibitors. The inhibition at 10 μM was higher for P-gp than for MRP1. Interestingly, the inhibition caused for both drugs at 10 μM on MRP1 was similar to the observed toward ABCG2 (~ 25 %). Both drugs completely inhibited P-gp and MRP1 at 100 μM . Using calcein-AM (Telbisz et al., 2021) or doxorubicin (Bierman et al., 2010) as substrate, ivermectin and lopinavir were also able to inhibit P-gp and MRP1. It was recently described that hydroxychloroquine at concentrations higher than 10 μM inhibits the P-gp activity, without effect on ABCG2 activity (Weiss et al., 2020). Here, we observed that both chloroquine and hydroxychloroquine inhibited the P-gp activity at 100 μM (see supplementary information Figure 1) without effect on ABCG2 (Figure 2A). In general terms, despite the search for specific inhibitors, the identification of dual- and pan-inhibitors is attractive (Zattoni et al., 2022a). In fact, the clinic trials failure of specific P-gp inhibitors was partially attributed to the overlap of transported substrates among the ABC transporters (Tamaki et al., 2011; Robey et al., 2018). Taken together, we confirmed that lopinavir and ivermectin act as pan-inhibitors of ABC transporters at 100 μM (Figure 2A, see supplementary information Figures 1 and 2).

High cytotoxicity and absence of ABCG2-mediated transport of lopinavir and ivermectin

To further investigate the interaction of the eight drugs with ABCG2, a cell viability assay was performed using HEK293 cells and transfected cells overexpressing ABCG2 (HEK292-*ABCG2*). Many classes of ABCG2

inhibitors also are recognized as ABCG2 substrates, and this effect can be initially investigated by a cell viability assay (Zattoni et al., 2022a). However, this approach is only useful for cytotoxic drugs. A lower cytotoxic effect triggered by drugs on cells overexpressing the ABC transporter than on the parental cell line suggests a transport. Since SN38 (the active metabolite of irinotecan) is a substrate of ABCG2, this drug was used as control. As shown in Figure 3, SN38 was transported by ABCG2, showing a lower cytotoxic effect on cells overexpressing ABCG2. All drugs decreased the cell viability after 72 hours of exposure. Some of these drugs, such as oseltamivir showed a very low cytotoxic effect, decreasing the cell viability only in concentrations higher than 200 μM (Figure 3H). In sharp contrast, lopinavir and ivermectin were highly cytotoxic, decreasing the cell viability at 12 and 3 μM , respectively (Figure 3D and E). Interestingly, the two drugs that inhibited ABCG2 transport activity also were the most cytotoxic agents.

The cytotoxic effect is an important parameter to be considered during the identification of ABCG2 inhibitors since many potent inhibitors did not follow pre-clinical studies due to their high intrinsic cytotoxicity (Boumendjel et al., 2011; Zattoni et al., 2022a). To correlate the inhibition potency and cytotoxicity, the inhibitors were compared based on their therapeutic rate (IG_{50}/IC_{50}), where the IG_{50} value is the concentration that decreases 50 % cell viability. In this way, compounds that present a high therapeutic rate (TR), such as chromone 6g (MBL-II-141), that showed a TR of 2000 (Valdameri et al., 2012b), are considered promising to be explored in pre-clinical models and clinical trials studies (Zattoni et al., 2022a). Here, the calculated TR for lopinavir and ivermectin were 0.64 and 0.26, respectively (see supplementary information Table 1). These very low TR values indicate that both compounds were highly cytotoxic and probably the ABCG2 inhibition effect might not be validated in animal models. However,

considering a drug repurposing strategy, another parameter that should be considered is the drug plasma concentration. The highest plasma concentrations described for lopinavir and ivermectin were 15 μM (https://www.accessdata.fda.gov/drugsatfda_docs/label/2007/021226s018lbl.pdf) and 53 nM (https://www.accessdata.fda.gov/drugsatfda_docs/label/2009/050742s026lbl.pdf), respectively. Thus, the clinical use of ivermectin as an ABCG2 inhibitor is impracticable, however, the IC_{50} value of ABCG2 inhibition of

lopinavir is in the same order magnitude of the plasma concentrations (μM range). Considering that the most promising ABCG2 inhibitor identified by the drug repurposing strategy is the febuxostat (Miyata et al., 2016; Toyoda et al., 2019), showing a IC_{50} of 27 nM and plasma concentration of 90 nM, its use in clinical dose possibly inhibits ABCG2 (Toyoda et al., 2019). In accordance, we found that ABCG2 is possibly inhibited by lopinavir in clinical dose.

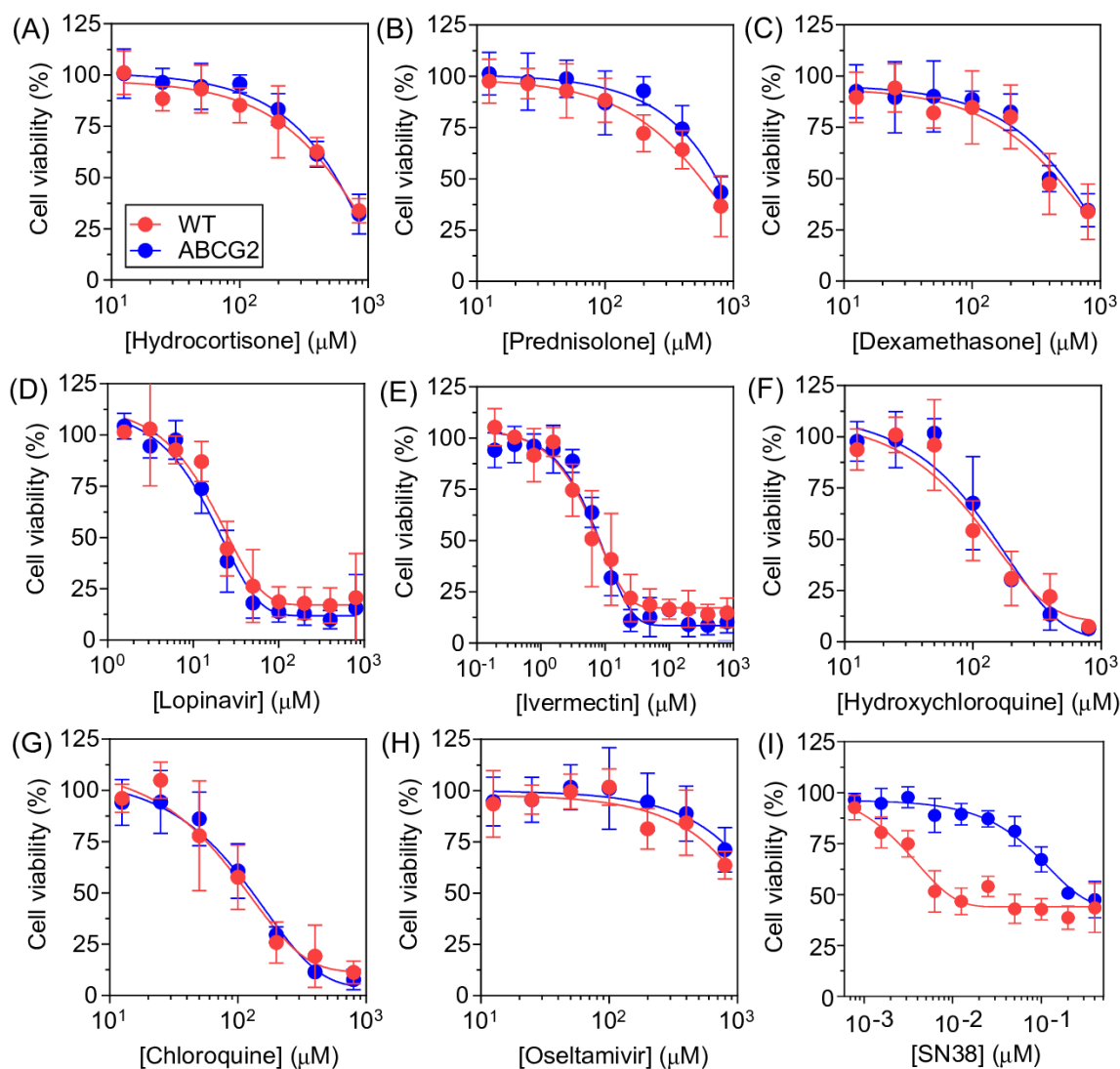


Figure 3: Cytotoxicity and absence of transport mediated by ABCG2 transporter. MTT cell viability assay was performed on HEK293 cells (WT) in red and HEK293-ABCG2 cells (ABCG2) in blue after 72 hours of treatment with (A) hydrocortisone, (B) prednisolone, (C) dexamethasone, (D) lopinavir, (E) ivermectin, (F) hydroxychloroquine, (G) chloroquine, (H) oseltamivir, and (I) SN38. Drugs were tested at different concentrations, as indicated in the graphs and the data represent the mean \pm SD of at least three independent experiments. Cells treated with the vehicle (DMSO or H_2O) were considered 100 % of viable cells.

Regarding the cytotoxic profile of the eight drugs comparing both cell lines, HEK293 and HEK293-*ABCG2*, no difference was evidenced (Figure 3). These results suggest that none of these drugs are recognized as substrates of *ABCG2* transporter. Our data further confirmed that hydroxychloroquine and lopinavir are not substrate for *ABCG2* (Agarwal et al., 2007; Bierman et al., 2010; Weiss et al., 2020). The absence of transport mediated by the target transporter is a desirable feature of inhibitors, which shows that lopinavir and ivermectin chemical structures promising scaffolds for the rational design of more potent *ABCG2* inhibitors.

Although the efflux mediated by P-gp of hydrocortisone (Nakayama et al. 1999), hydroxychloroquine (Weiss et al., 2020), lopinavir (Agarwal et al., 2007), dexamethasone (Ueda et al., 1992), oseltamivir (Morimoto et al., 2008), prednisolone (Karssen et al., 2002) and ivermectin (Didier and Loor 1995) has been described, we decided to evaluate the transport of all drugs by the MTT-based cell viability assay using parental and a cell line overexpressing P-gp. Ivermectin, dexamethasone and oseltamivir behaved as P-gp substrates, whereas hydrocortisone, prednisolone, lopinavir, hydroxychloroquine and chloroquine did not (see supplementary information Figure 3). Using the same approach for MRP1, we found that oseltamivir was the only drug not recognized as substrate. Lopinavir could be considered as strong substrate, whereas ivermectin could be considered as weak substrate (see supplementary information Figure 4). Ivermectin, chloroquine and dexamethasone have already been described as MRP1 substrates (Vezmar and Georges, 1998; Ardelli, 2013; Aberuyi et al., 2021; Rendic, 2021), while prednisolone and lopinavir have been described as non-substrates (Webster and Carlstedt-Duke, 2002; Bierman et al., 2010). In summary, our data confirmed that many drugs that were used for COVID-19 interact with the main ABC transporters involved in MDR, being inhibitors or substrates, and in some cases, the

inhibitor is also transported, such as ivermectin on P-gp.

Mechanism of ABCG2 inhibition exploited by in vitro approaches

Since lopinavir and ivermectin inhibited *ABCG2*, and the IC_{50} value of *ABCG2* inhibition caused by lopinavir is in the same order of magnitude of the plasma concentration, the molecular mechanism of inhibition was studied. The interaction of drugs with ABC transporters can be studied by different *in vitro* approaches, including the use of conformational antibodies (Zattoni et al., 2022a). In the case of *ABCG2* transporter, the antibody called clone 5D3 recognizes an extracellular epitope of the protein (Taylor et al., 2017). In general, *ABCG2* inhibitors induce a conformational change that increases the 5D3 binding, in contrast to *ABCG2* substrates, which do not trigger this “5D3 shift” (Telbisz et al., 2012; Zattoni et al., 2022a). Lopinavir and ivermectin induced an increase in 5D3 binding, such as the *ABCG2* reference inhibitor Ko143 (Figure 4A). As shown by the histograms, the 5D3 shift is more pronounced for lopinavir and ivermectin than Ko143 (Figure 4B). This result agrees with our previous data that demonstrated that lopinavir and ivermectin are non-transported inhibitors of *ABCG2* (Figures 2 and 3).

Drugs that inhibit the transport activity of ABC transporters are called functional inhibitors. This inhibition effect is settled on the direct binding of ligands in a druggable binding pocket of these transporters, commonly located at transmembrane domains (Kowal et al., 2021; Zattoni et al., 2022a). However, drugs targeting transcriptional or posttranslational protein levels have been described as promising to overcome the MDR phenotype. Drugs that trigger this effect are considered modulators, to differentiate functional inhibitors. In addition, a dual effect, direct transport inhibition and decreased protein levels are advantageous but poorly observed (Zattoni et al., 2022a). Here, the effect of lopinavir and ivermectin on *ABCG2* was tested at transcriptional and translational levels, by qPCR and

western blot, respectively. Considering a half-life of approximately 60 hours for ABCG2 in different cell lines (Imai et al., 2009; Peng et al., 2010), both assays were performed after 72 hours of drug exposure. In addition, to avoid a bias associated with the cytotoxicity effect, the highest drug concentration that does not decrease the cell viability was used to treat the cells. In this case, 6.25 and 1.56 μM for lopinavir and ivermectin, respectively (Figure 3D and E). As shown in Figure 4C, lopinavir and ivermectin did not modulate the mRNA expression levels of ABCG2. The western blot results also revealed an absence of effect of both drugs on protein expression levels (Figure 4D). Together, these data confirm that lopinavir and ivermectin are not modulators of ABCG2 expression levels and should be classified as functional inhibitors of ABCG2.

To get insights into the biochemical mechanism of ABCG2 inhibition, the type of inhibition caused by ivermectin and lopinavir was investigated by varying the concentrations of the inhibitor and the substrate mitoxantrone. This ABCG2 substrate was used instead of Hoechst 33342 because only with mitoxantrone a saturation curve was achieved (Figure 5A and C). Both drugs caused a non-competitive inhibition since an increase of V_{max} with no effect on K_M value was observed (Figure 5B and D). The ABCG2 noncompetitive inhibition was already reported by some compounds, such as stilbene derivatives (Valdameri et al., 2012c). Recently, an uncompetitive and mixed-type of inhibition were also described for indenoindole (Guragossian et al., 2021) and porphyrins, respectively (Zattoni et al., 2022b).

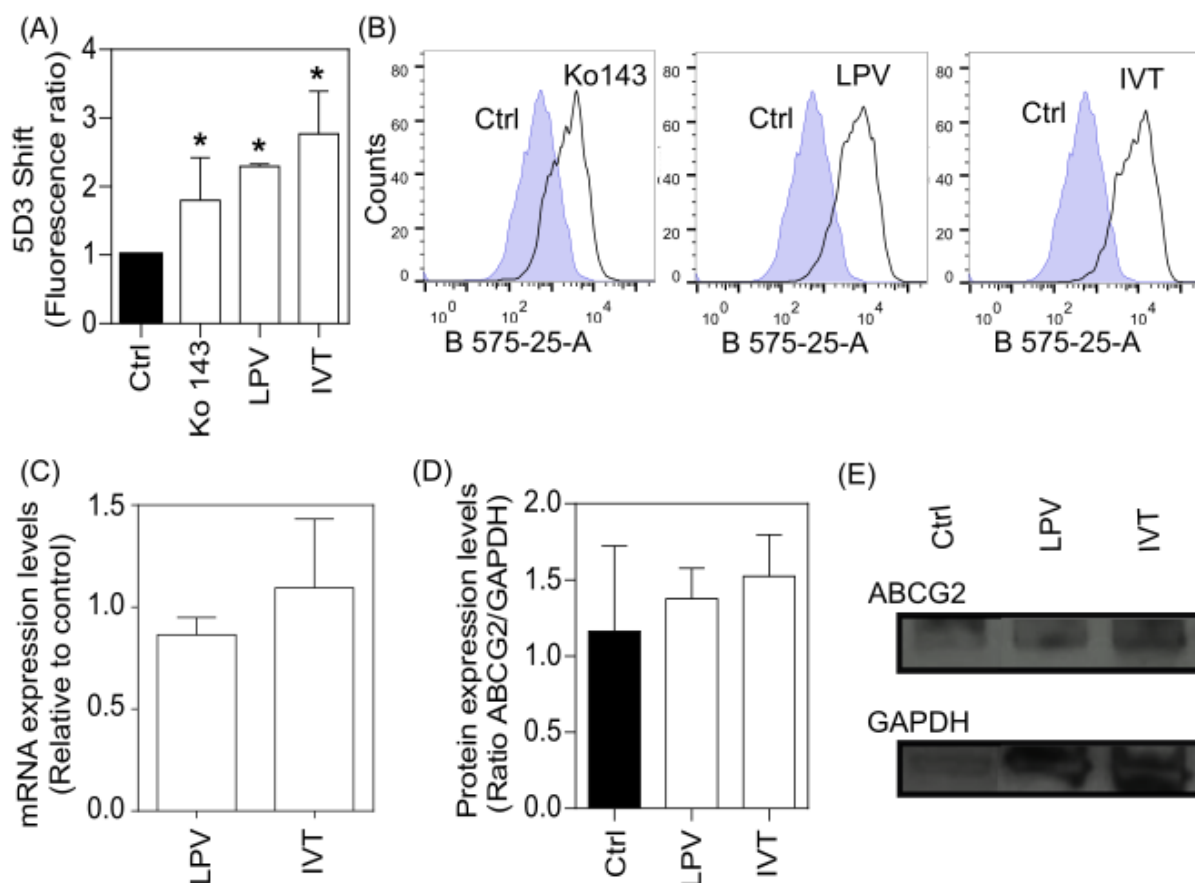


Figure 4: ABCG2 inhibition by flow cytometry. **(A)** Conformational 5D3 antibody binding. The data was normalized by the untreated control. *Significant difference ($p > 0.05$) according to Kruskal-Wallis test comparing the different groups (Ctrl, Ko143, LPV and IVT). **(B)** Representative histograms of “5D3 shift” assay: Ko143 (1 μM), lopinavir (100 μM) and ivermectin (100 μM) conditions. **(C)** mRNA expression levels quantified by qPCR. **(D)** Protein expression levels quantified by western blot. **(E)** Representative image of western blot assay.

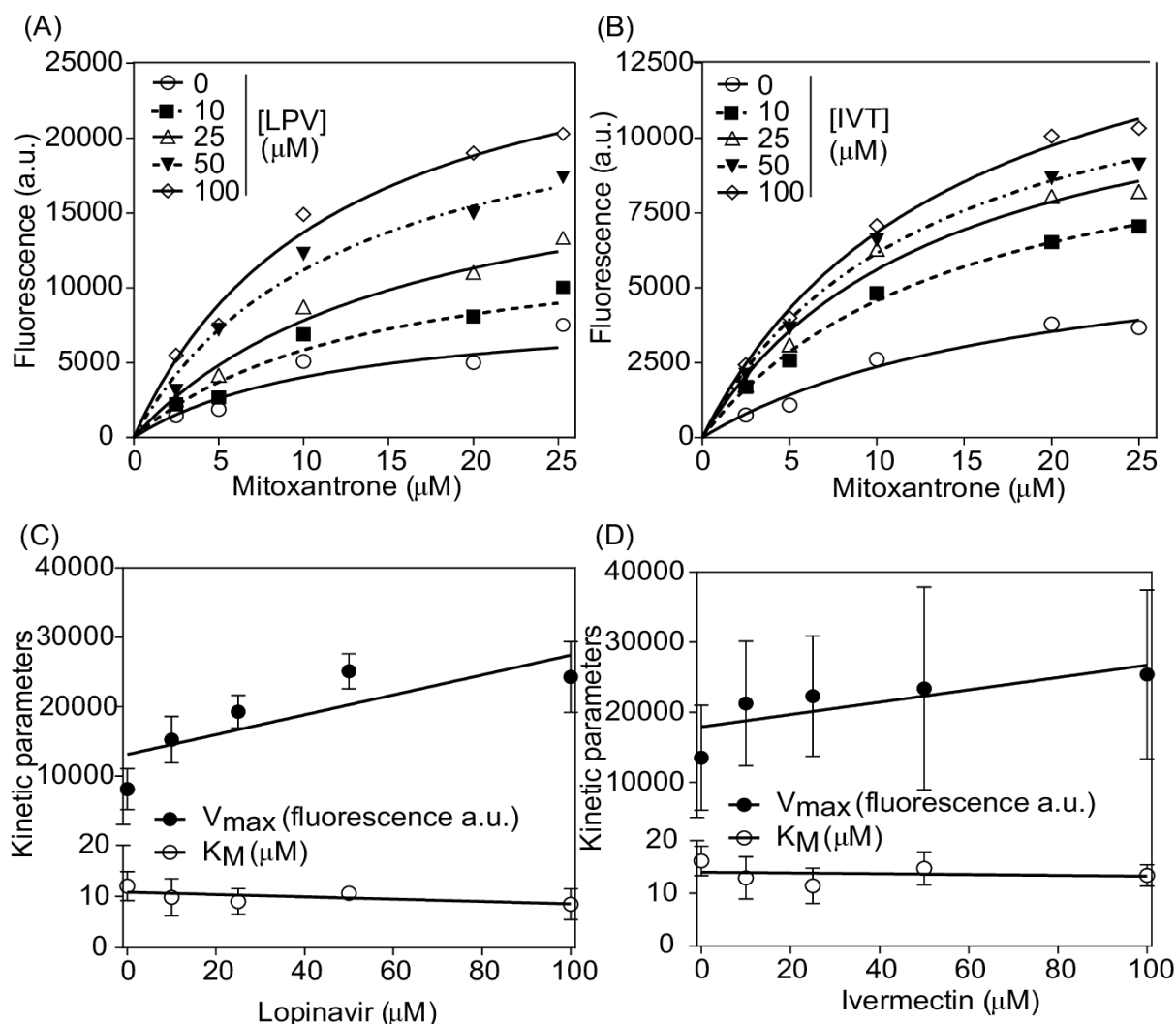


Figure 5: Kinetic behavior of mitoxantrone ABCG2-mediated efflux by flow cytometry. Intracellular fluorescence was determined using a range of mitoxantrone/inhibitors concentrations. (A) Lopinavir (LPV). (B) Ivermectin (IVT). Comparison of V_{max} and K_M of (C) lopinavir and (D) ivermectin. Data represent the mean ± SD of at least three independent experiments.

Molecular docking and dynamic simulations

In order to gain further insights into the noncompetitive inhibition caused by lopinavir and ivermectin, *in silico* analyses were performed using molecular docking, molecular dynamics and MM/GBSA free binding energy calculations. Initially, molecular docking analysis showed a compatibility of the binding of inhibitors lopinavir and ivermectin in presence of the substrate mitoxantrone, revealing multiple conformations of each ligand co-occupying the drug binding cavity (DBC). The results suggested that the large DBC, lo-

cated between both subunits of transmembrane helices, can accommodate one molecule of mitoxantrone and one molecule of each inhibitor simultaneously (Figure 6). Analysis of the docked complex showed that mitoxantrone occupied an “upper” position, closer to the L554/L555 plug, but ivermectin and lopinavir occupied a “below” position, closer of the cytoplasmic side (Figure 6).

To further investigate the stability of the complex ligands-ABCG2 and specific types of interaction and other potential binding modes, molecular dynamics (MD) simulations were performed. The results were simi-

lar to those observed by docking (see supplementary information Figure 5). Mitoxantrone acted similarly in the presence or absence of an inhibitor, basically conserving the high frequency of F439/N436 interactions. The binding free energies (ΔG_{bind}) estimated revealed that the binding of ivermectin or lopinavir does not significantly alter the mitoxantrone binding affinity (Figure 6A). Docking results initially showed that the most common interaction between ABCG2 transporter and mitoxantrone involves a π -stacking with F439 (Figure 6). MD results confirmed this observation and mitoxantrone binding was mainly favored by π -stacking interactions between the anthracenedione core of mitoxantrone and

F439, as well by H-bonds with N436 from both subunits. The lack of interactions between mitoxantrone and ivermectin revealed by docking results was further elucidated by MD, which showed frequent water-mediated H-bonds present between the tetrahydropyran moiety of ivermectin and E446 (Figure 6B and C). This amino acid residue also interacted with lopinavir, indicating an important role in the stabilization of these inhibitors inside the drug pocket in presence of mitoxantrone. Together, these results suggest an absence of overlap between inhibitors and mitoxantrone, providing a plausible explanation for the noncompetitive inhibition.

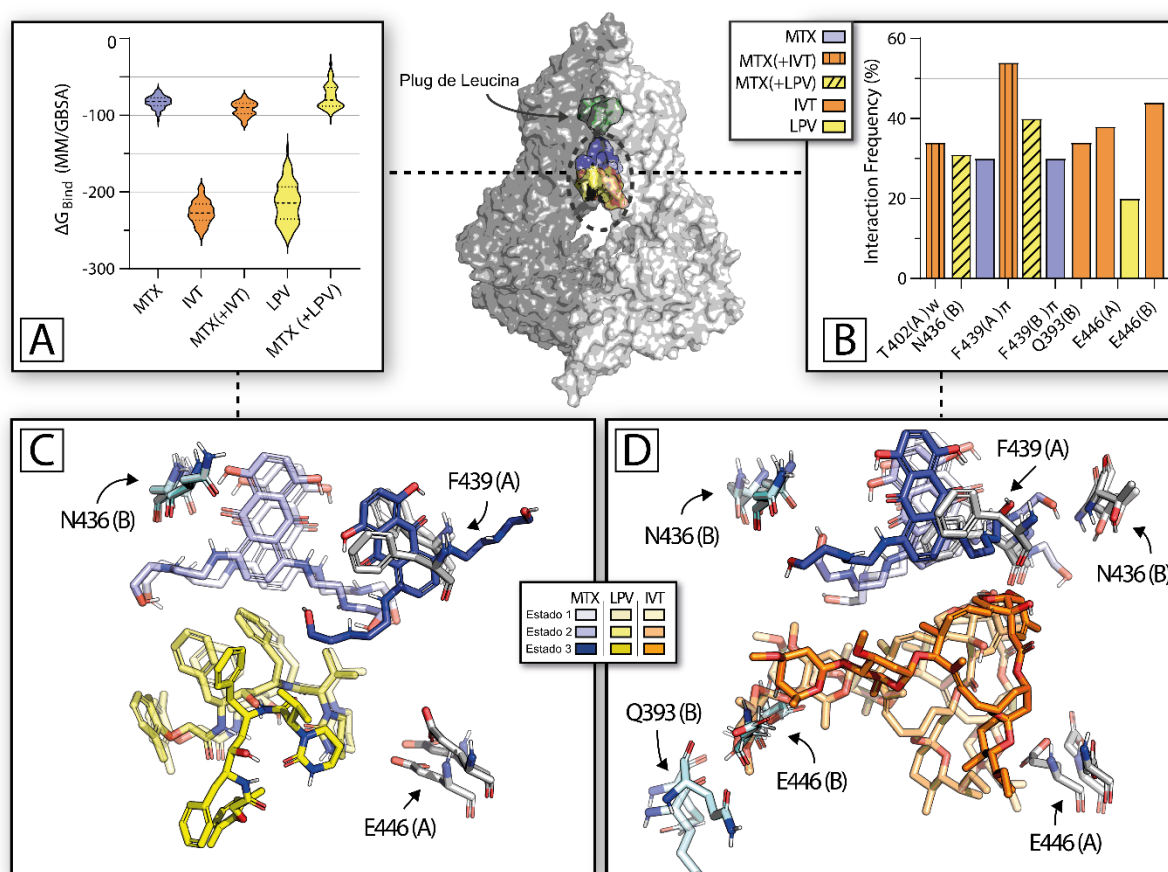


Figure 6: Molecular docking and molecular dynamics simulations. **(A)** The violin plot shows calculated binding affinity (kcal/mol) of MTX and MTX (+ inhibitor) complexes. **(B)** Bar chart, with interaction frequency (fraction of simulation time) between important residues and each molecule. **(C and D)** Sticks representation of three most prevalent populations of IVT (shades of orange), LPV (shades of yellow) and MTX (shades of blue). Residues with frequent interactions are indicated with arrows. Oxygen and nitrogen atoms are colored red and blue, respectively, and non-polar hydrogens are omitted. In the center: Surface representation of 6VXI and ligands in State 1, indicating the DBC, delimited by the leucine 554/555 plug (colored in pale green). MTX is mitoxantrone; LPV is lopinavir and IVT is ivermectin.

Furthermore, analysis of root-mean-square deviation (RMSD) values via a clustering algorithm showed three states in proximity for each inhibitor, indicating a low variation in terms of mobility inside the drug-binding pocket of ABCG2 (Figure 6C and D). These data suggest that binding of a second molecule, in this case, an inhibitor, cannot displace mitoxantrone from the DBC. In accordance, previous works of MD simulations using cryo-EM obtained structures strongly suggests that ligands can alter the protein conformation, allowing a simultaneous binding of substrates and inhibitors (Nagy et al., 2020; Yu et al., 2021).

Previous reports suggest that F439 is critical for the binding and stabilization of substrates by clamping the molecule inside the cavity (Gose et al., 2020), and mutations at position 439 severely impair Hoechst 33342 and pheophorbide *a* (Gose et al., 2020). Interestingly, the importance of N436 appears to be more specific and dependent on the molecule (Gose et al., 2020; Kowal et al., 2021), is indispensable for mitoxantrone transport (Guragossian et al., 2021). The importance of E446 for ABCG2 function was also confirmed by mutagenesis studies (Khunweeraphong et al., 2017; Szöllösi et al., 2019). Our data suggest that mitoxantrone binds to the F436 region, while the inhibitors were trapped between E446 residues, blocking the proximity of transmembrane domains needed for the catalytic cycle of transport mediated by ABCG2. This spatial configuration allows these inhibitors to act as a wedge, preventing the approach of transmembrane helices necessary to attain turnover conformations that potentially precede substrate efflux to the extracellular space (Yu et al., 2021), but not avoiding substrate accommodation inside the DBC. However, a complete understanding of the catalytic cycle and drug dislocation from cavity 1 (drug binding pocket) to cavity 2 (above the L555), as well as the conformational changes induced by these inhibitors require additional studies.

CONCLUSION

Our results confirmed that lopinavir and ivermectin are functional inhibitors of ABCG2, P-gp and MRP1. Here, for the first time, we characterize the molecular mechanism of ABCG2 inhibition by lopinavir and ivermectin using cell-based and *in silico* approaches. Both drugs were not recognized as substrates and did not affect the mRNA and protein expression levels. In addition, lopinavir and ivermectin increased the binding of antibody 5D3, such as the reference inhibitor Ko143. Both compounds caused a noncompetitive inhibition, binding in a different site than mitoxantrone, as also confirmed by molecular docking, dynamic simulations followed by free energy calculations. Thus, the data shows that lopinavir is a potent ABCG2 inhibitor at maximum plasma concentrations and both lopinavir and ivermectin can be used as scaffolds for the design more powerful ABCG2 inhibitors.

Acknowledgment

We thank Dr Attilio Di Pietro from IBCP (France), Dr Robert W. Robey and Dr Michael Gottesman from NCI/NIH (USA) for having provided the cell lines. This work was supported by PROIND 2020 (UFPR), Fundação Araucária/PPSUS (grant number 2020131000003) and Coordenação de Aperfeiçoamento de Pessoal de Nível Superior – Brasil (CAPES) (Finance code 001). The authors would like to thank the Finnish IT center for science (CSC), Ltd. for the generous computational resources. The study was financially supported by the TüCAD2, a program funded by the Federal Ministry of Education and Research (BMBF) and the Baden-Württemberg Ministry of Science as part of the Excellence Strategy of the German Federal and State Governments (TK). In addition, TK was funded by the Fortüne grant initiative under the Excellence Strategy.

Declaration of competing interest

The authors declare that they have no conflict of interest.

REFERENCES

- Aberuyi N, Rahgozar S, Pourabutaleb E, Ghaedi K. Selective dysregulation of ABC transporters in methotrexate-resistant leukemia T-cells can confer cross-resistance to cytarabine, vincristine and dexamethasone, but not doxorubicin. *Curr Res Transl Med.* 2021;69:103269.
- Agarwal S, Pal D, Mitra AK. Both P-gp and MRP2 mediate transport of lopinavir, a protease inhibitor. *Int J Pharm.* 2007;339:139–47.
- Ali H, Du Z, Li X, Yang Q, Zhang YC, Wu M, et al. Identification of suitable reference genes for gene expression studies using quantitative polymerase chain reaction in lung cancer in vitro. *Mol Med Rep.* 2015;11:3767–73.
- Allen JD, van Loevezijn A, Lakhai JM, van der Valk M, van Tellingen O, Reid G, et al. Potent and specific inhibition of the breast cancer resistance protein multidrug transporter in vitro and in mouse intestine by a novel analogue of fumitremorgin C. *Mol Cancer Ther.* 2002;1:417–25.
- Allikmets R, Schriml LM, Hutchinson A, Romano-Spica V, Dean M. A human placenta-specific ATP-binding cassette gene (ABCP) on chromosome 4q22 that is involved in multidrug resistance. *Cancer Res.* 1998;58:5337–9.
- Ardelli BF. Transport proteins of the ABC systems superfamily and their role in drug action and resistance in nematodes. *Parasitol Int.* 2013;62:639–46.
- Bierman WFW, Scheffer GL, Schoonderwoerd A, Jansen G, Van Agtmael MA, Danner SA, et al. Protease inhibitors atazanavir, lopinavir and ritonavir are potent blockers, but poor substrates, of ABC transporters in a broad panel of ABC transporter-overexpressing cell lines. *J Antimicrob Chemother.* 2010;65:1672–80.
- Boumendjel A, Macalou S, Valdameri G, Pozza A, Gauthier C, Arnaud O, et al. Targeting the multidrug ABCG2 transporter with flavonoidic inhibitors: *In vitro* optimization and *in vivo* validation. *Curr Med Chem.* 2011;18:3387–401.
- Bowers KJ, Chow E, Xu H, Dror RO, Eastwood MP, Gregersen BA, et al. Scalable algorithms for molecular dynamics simulations on commodity clusters. In: *SC '06: Proceedings of the 2006 ACM/IEEE Conference on Supercomputing*, Tampa, FL, USA, 2006 (pp 43–43). doi: 10.1109/SC.2006.54.
- Darden T, York D, Pedersen L, Darden T, York D, Pedersen L. Particle mesh Ewald : An Nlog (N) method for Ewald sums in large systems Particle mesh Ewald : An N -log (N) method for Ewald sums in large systems. *J Chem Phys.* 1993;98:10089.
- Dean M, Rzhetsky A, Allikmets R. The human ATP-binding cassette (ABC) transporter superfamily. *Genome Biol.* 2001;11:1156–66.
- Didier AD, Loor F. Decreased biotolerability for ivermectin and cyclosporin a in mice exposed to potent P-glycoprotein inhibitors. *Int J Cancer.* 1995;63:263–7.
- Doyle LA, Yang W, Abruzzo LV, Kroghmann T, Gao Y, Rishi AK, et al. A multidrug resistance transporter from human MCF-7 breast cancer cells. *Proc Natl Acad Sci U S A.* 1998;95:15665–70.
- Eberhardt J, Santos-martins D, Tillack AF, Forli S. AutoDock Vina 1.2.0: New docking methods, expanded force field, and python bindings. *J Chem Inf.* 2021;61:3891–8.
- Gose T, Allcock A, Tamai I, Shafi T, Fukuda Y, Das S, et al. ABCG2 requires a single aromatic amino acid to “clamp” substrates and inhibitors into the binding pocket. *FASEB J.* 2020;34:4890–4903.
- Gottesman MM. Mechanisms of cancer drug resistance. *Annu Rev Med.* 2002;53:615–27.
- Gottesman MM, Fojo T, Bates SE. Multidrug resistance in cancer: Role of ATP-dependent transporters. *Nat Rev Cancer.* 2002;2:48–58.
- Gottesman MM, Lavi O, Hall MD, Gillet J. Toward a better understanding of the complexity of cancer drug resistance. *Rev Pharmacol Toxicol.* 2016;56:85–102.
- Guragossian N, Belhani B, Moreno A, Nunes MT, Gonzalez-Lobato L, Marminon C, et al. Uncompetitive nanomolar dimeric indenoindole inhibitors of the human breast cancer resistance pump ABCG2. *Eur J Med Chem.* 2021;211:113017.
- Halgren TA. MMFF VI. MMFF94s option for energy minimization studies. *J Comput Chem.* 1999;20:720–9.
- Halgren TA, Nachbar RB. Conformational energies and geometries for MMFF94. *J Comput Chem.* 1996;17:587–615.
- Hall MD, Handley MD, Gottesman MM. Is resistance useless? Multidrug resistance and collateral sensitivity. *Trends Pharmacol Sci.* 2009;30:546–56.

- Imai Y, Ohmori K, Yasuda S, Wada M, Suzuki T, Fukuda K, et al. Breast cancer resistance protein/ABCG2 is differentially regulated downstream of extracellular signal-regulated kinase. *Cancer Sci.* 2009;100:1118–27.
- Jacob F, Guertler R, Naim S, Nixdorf S, Fedier A, Hacker NF, et al. Careful selection of reference genes is required for reliable performance of RT-qPCR in human normal and cancer cell lines. *PLoS One.* 2013;8:e59180.
- Jacobson MP, Pincus DL, Rapp CS, Day T, Honig B, Shaw DE, et al. A hierarchical approach to all-atom protein loop prediction. *Proteins.* 2004;367:351–67.
- Jani M, Makai I, Kis E, Szabó P, Nagy T, Krajcsi P, et al. Ivermectin interacts with human ABCG2. *J Pharm Sci.* 2011;100:94–7.
- Jorgensen WL, Chandrasekhar J, Madura JD, Impey RW, Klein ML, Jorgensen WL, et al. Comparison of simple potential functions for simulating liquid water. *J Chem Phys.* 1983;926-35.
- Juvale K, Wiese M. Design of inhibitors of BCRP/ABCG2. *Future Med Chem.* 2015;7:1521–7.
- Karssen A, Meijer O, Van Der Sandt I, De Boer A, De Lange E, De Kloet E. The role of the efflux transporter P-glycoprotein in brain penetration of prednisolone. *J Endocrinol.* 2002;175:251–60.
- Khunweeraphong N, Stockner T, Kuchler K. The structure of the human ABC transporter ABCG2 reveals a novel mechanism for drug extrusion. *Sci Rep.* 2017;7:13767.
- Kita DH, Guragossian N, Zattoni IF, Moure VR, Rego FG de M, Lusvardi S, et al. Mechanistic basis of breast cancer resistance protein inhibition by new indeno[1,2-b]indoles. *Sci Rep.* 2021;11:1788.
- Kowal J, Ni D, Jackson SM, Manolaridis I, Stahlberg H, Locher KP. Structural basis of drug recognition by the multidrug transporter ABCG2. *J Mol Biol.* 2021;433:1–48.
- Lemma S, Avnet S, Salerno M, Chano T, Baldini N. Identification and validation of housekeeping genes for gene expression analysis of cancer stem cells. *PLoS One.* 2016;11:e0149481.
- Lu C, Wu C, Ghoreishi D, Chen W, Wang L, Damm W, et al. OPLS4: Improving force field accuracy on challenging regimes of chemical space. *J Chem Theory Comput.* 2021;17:4291–300.
- Miyake K, Mickley L, Litman T, Zhan Z, Robey R, Cristensen B, et al. Molecular cloning of cDNAs which are highly overexpressed in mitoxantrone-resistant cells. *Cancer Res.* 1999;59:8–13.
- Miyata H, Takada T, Toyoda Y, Matsuo H, Ichida K, Suzuki H. Identification of febuxostat as a new strong ABCG2 inhibitor: Potential applications and risks in clinical situations. *Front Pharmacol.* 2016;7:518.
- Morimoto K, Nakakariya M, Shirasaka Y, Kakinuma C, Fujita T, Tamai I, et al. Oseltamivir (Tamiflu) efflux transport at the blood-brain barrier via P-glycoprotein. *Drug Metab Dispos.* 2008;36:6–9.
- Morris GM, Huey R, Lindstrom W, Sanner MF, Belew RK, Goodsell DS, et al. AutoDock4 and AutoDockTools4: Automated docking with selective receptor flexibility. *J Comput Chem.* 2009;30:2785–91.
- Nagy T, Tóth Á, Telbisz Á, Sarkadi B, Tordai H, Tordai A. The transport pathway in the ABCG2 protein and its regulation revealed by molecular dynamics simulations. *Cell Mol Life Sci.* 2020;78:2329–39.
- Nakayama A, Eguchi O, Hatakeyama M, Saitoh H, Takada M. Different absorption behaviors among steroid hormones due to possible interaction with P-glycoprotein in the rat small intestine. *Biol Pharm Bull.* 1999;22:535–8.
- Orlando BJ, Liao M. ABCG2 transports anticancer drugs via a closed-to-open switch. *Nat Commun.* 2020;11:2264.
- Peng H, Qi J, Dong Z, Zhang JT. Dynamic vs static ABCG2 inhibitors to sensitize drug resistant cancer cells. *PLoS One.* 2010;5:15276.
- Pfaffl MW. A new mathematical model for relative quantification in real-time RT-PCR. *Nucleic Acids Res.* 2001;29:e45.
- Potashnikova D, Gladkikh A, Vorobjev IA. Selection of superior reference genes combination for quantitative real-time PCR in B-cell lymphomas. *Ann Clin Lab Sci.* 2015;45:64–72.
- Rabindran SK, He H, Singh M, Brown E, Collins KI, Annable T, et al. Reversal of a novel multidrug resistance mechanism in human colon carcinoma cells by fumitremogin C. *Cancer Res.* 1998;58:5850–8.
- Rendic SP. Metabolism and interactions of Ivermectin with human cytochrome P450 enzymes and drug transporters, possible adverse and toxic effects. *Arch Toxicol.* 2021;95:1535–46.

- Robey RW, Pluchino KM, Hall MD, Fojo AT, Bates SE, Gottesman MM. Revisiting the role of ABC transporters in multidrug-resistant cancer. *Nat Rev Cancer*. 2018;18:452–64.
- Saidova AA, Potashnikova DM, Tvorogova AV, Maly IV, Hofmann WA, Vorobjev IA. Specific and reliable detection of myosin 1c isoform a by RTqPCR in prostate cancer cells. *PeerJ*. 2018;6:e5970.
- Sharan RN, Vaiphei ST, Nongrum S, Keppen J, Ksoo M. Consensus reference gene(s) for gene expression studies in human cancers: end of the tunnel visible? *Cell Oncol*. 2015;38:419–31.
- Shim JS, Liu JO. Recent advances in drug repositioning for the discovery of new anticancer drugs. *Int J Biol Sci*. 2014;10:654.
- Sterling T, Irwin JJ. ZINC 15 – Ligand discovery for everyone. *J Chem Inf Model*. 2015;55:2324–37.
- Stewart JJP. MOPAC ((Molecular Orbital PACKage). Stewart Computational Chemistry. MOPAC2016. <http://OpenMOPAC.net>. 2016.
- Szakács G, Paterson JK, Ludwig JA, Booth-Genthe C, Gottesman MM. Targeting multidrug resistance in cancer. *Nat Rev Drug Discov*. 2006;5:219–34.
- Szakács G, Hall MD, Gottesman MM, Boumendjel A, Kachadourian R, Day BJ, et al. Targeting the achilles heel of multidrug-resistant cancer by exploiting the fitness cost of resistance. *Chem Rev*. 2014;114:5753–74.
- Szöllösi NKD, Stockner T, Kuchler K. The ABCG2 multidrug transporter is a pump gated by a valve and an extracellular lid. *Nat Commun*. 2019;10:5433.
- Tamaki A, Ierano C, Szakacs G, Robey RW, Bates SE, Branch O, et al. The controversial role of ABC transporters in clinical oncology. *Essays Biochem*. 2011;50:209–32.
- Taylor NMI, Manolaridis I, Jackson SM, Kowal J, Stahlberg H, Locher KP. Structure of the human multidrug transporter ABCG2. *Nature*. 2017;7:13767.
- Telbisz Á, Hegedüs C, Özvegy-Laczka C, Goda K, Várady G, Takáts Z, et al. Antibody binding shift assay for rapid screening of drug interactions with the human ABCG2 multidrug transporter. *Eur J Pharm Sci*. 2012;45:101–9.
- Telbisz Á, Ambrus C, Móznér O, Szabó E, Várady G, Bakos É, et al. Interactions of potential anti-COVID-19 compounds with multispecific ABC and OATP drug transporters. *Pharmaceutics*. 2021;13(1):81.
- Toyoda Y, Takada T, Suzuki H. Inhibitors of human ABCG2: From technical background to recent updates with clinical implications. *Front Pharmacol*. 2019;10:208.
- Ueda K, Okamura N, Hirai M, Tanigawara Y, Saeki T, Kioka N, et al. Human P-glycoprotein transports cortisol, aldosterone, and dexamethasone, but not progesterone. *J Biol Chem*. 1992;267:24248–52.
- Valdameri G, Gauthier C, Terreux R, Day BJ, Winnischofer SMB, Rocha MEM, et al. Investigation of chalcones as selective inhibitors of the breast cancer resistance protein: Critical role of methoxylation in both inhibition potency and cytotoxicity. *J Med Chem*. 2012a;55:3193–200.
- Valdameri G, Genoux-bastide E, Peres B, Gauthier C, Guitton J, Terreux R, et al. Substituted chromones as highly potent nontoxic inhibitors, specific for the breast cancer resistance protein. *J Med Chem*. 2012b;55:966–70.
- Valdameri G, Pereira Rangel L, Spatafora C, Guitton J, Gauthier C, Arnaud O, et al. Methoxy stilbenes as potent, specific, untransported, and noncytotoxic inhibitors of breast cancer resistance protein. *ACS Chem Biol*. 2012c;7:322–30.
- Vesga LC, Kronenberger T, Tonduru AK, Kita DH, Zattoni IF, Bernal CC, et al. Tetrahydroquinoline/4,5-Dihydroisoxazole molecular hybrids as inhibitors of breast cancer resistance protein (BCRP/ABCG2). *ChemMedChem*. 2021;16:2686–94.
- Vezmar M, Georges E. Direct binding of chloroquine to the multidrug resistance protein (MRP): Possible role for MRP in chloroquine drug transport and resistance in tumor cells. *Biochem Pharmacol*. 1998;56:733–42.
- Webster JI, Carlstedt-Duke J. Involvement of multidrug resistance proteins (MDR) in the modulation of glucocorticoid response. *J Steroid Biochem Mol Biol*. 2002;82:277–88.
- Weiss J, Rose J, Storch CH, Ketabi-Kiyanvash N, Sauer A, Haefeli WE, et al. Modulation of human BCRP (ABCG2) activity by anti-HIV drugs. *Antimicrob Chemother*. 2007;59:238–45.
- Weiss J, Bajraktari-Sylejmani G, Haefeli WE. Interaction of hydroxychloroquine with pharmacokinetically important drug transporters. *Pharmaceutics*. 2020;12(10):919.
- Yu Q, Ni D, Kowal J, Locher KP, Manolaridis I, Jackson SM, et al. Structures of ABCG2 under turnover conditions reveal a key step in the drug transport mechanism. *Nat Commun*. 2021;12:4376.

Zattoni IF, Delabio LC, Dutra J de P, Kita DH, Scheiffer G, Hembecker M, et al. Targeting breast cancer resistance protein (BCRP/ABCG2): Functional inhibitors and expression modulators. *Eur J Med Chem.* 2022a;237:114346.

Zattoni IF, Kronenberger T, Kita DH, Guanaes LD, Guimarães MM, de Oliveira Prado L, et al. A new porphyrin as selective substrate-based inhibitor of breast cancer resistance protein (BCRP/ABCG2). *Chem Biol Interact.* 2022b;351:109718.

Zhang C, Wang YQ, Jin G, Wu S, Cui J, Wang RF. Selection of reference genes for gene expression studies in human bladder cancer using SYBR-green quantitative polymerase chain reaction. *Oncol Lett.* 2017;14:6001–11.